

Entrance channel effects in nucleon and α particle preequilibrium decay of $^{63}\text{Cu}^*$ and $^{64}\text{Zn}^*$

R. Scherwinski, A. Alevra,* J. Friese, R. Langkau, and W. Scobel

I. Institut für Experimentalphysik, Universität Hamburg,

D-2000 Hamburg, Federal Republic of Germany

(Received 21 September 1981)

Double differential cross sections for the inclusive production of neutrons, protons, and α particles from ^{59}Co and ^{60}Ni bombarded with α particles of energies $E_\alpha=28$ and 32 MeV, respectively, have been measured for several angles between 15° and 160° . Hybrid model calculations for the preequilibrium decay consistently yield initial exciton numbers $n_0=5(4)$ for both neutron and proton emission from $\alpha+^{59}\text{Co}$ ($\alpha+^{60}\text{Ni}$) if pairing effects are taken into account. The angular distributions of nucleons and α particles differ from those of the reactions $p+^{62}\text{Ni}, ^{63}\text{Cu}$; they are discussed in the framework of the generalized exciton model that distinguishes between multistep direct and multistep compound contributions.

<p>NUCLEAR REACTIONS $^{59}\text{Co}, ^{60}\text{Ni}(\alpha, xn), (\alpha, xp), (\alpha, x\alpha), E_\alpha$ $=28-32$ MeV; measured $\sigma(E_y, \Theta_y)$, deduced $\sigma(E_y), y=n, p, \alpha$; calculated preequilibrium decay mode, deduced exciton configuration, entrance channel dependence.</p>
--

I. INTRODUCTION

Continuous spectra of light particles have been analyzed for more than ten years in terms of statistical models including preequilibrium (PE) decay modes. The exciton¹ and the hybrid² model succeeded in reproducing and predicting the angle integrated spectra of nucleons and, later on, also of more complex particles. In the last few years these semiclassical models have been extended³⁻⁶ to allow the calculation of double differential cross sections $d^2\sigma/d\Omega d\epsilon$. In a different approach, Tamura *et al.*⁷ performed a microscopic description for the first two steps of a multistep direct reaction populating the continuum that was based on the formalism for transitions to isolated residual states. A very promising approach is the one of Feshbach *et al.*⁸ It distinguishes between two classes of transitional states during the equilibration that are chained and contribute incoherently to the total cross section: the multistep direct (MSD) and the multistep compound (MSC) part.

Chiang and Hüfner⁹ have stressed that all these models, in spite of their different physical ingredients, agree to within a factor of 2. They trace this agreement back to a correct treatment of the dominating first few collisions in all models. For

the semiclassical models mentioned above this implies the correct choice of the initial exciton number n_0 . This question seems to be settled for nucleon, deuteron, and ^3He projectiles¹⁰⁻¹²; for α particles, values $n_0=3-5$ are reported for (α, n) or (α, p) reactions^{10,13} with an indication of a dependence on the odd-even character of the reaction system.^{14,15}

Calculations in the framework of the MSD/MSC model have been performed with good success^{16,17}; unfortunately they are very time consuming. Therefore Kalbach¹⁸ has extended the exciton model in a way that it allows a separation into MSD and MSC contributions, and has deduced the shape of their angular distributions with a phenomenological approach. This pragmatic procedure leads to a number of predictions on the entrance and exit channel (in)dependence of the angular distributions.¹⁹

The present work is devoted to a determination of n_0 for α induced reactions and a test of the extended exciton model in the mass $A \approx 60$ region. We report on measurements of double differential cross sections $d^2\sigma/d\Omega d\epsilon$ for the α induced reactions on $^{59}\text{Co}, ^{60}\text{Ni}$ with 28 and 32 MeV projectiles and for the neutron, proton, and α exit channels. Experimental details and results are given in Sec. II. From the simultaneous analysis of the angle in-

egrated spectra of both nucleon exit channels we expect constraints for a consistent description of the initial configuration taking into account the odd-even character and the influence of pairing corrections (Sec. III). The angular distributions of neutrons, protons, and α particles provide a test of the phenomenological MSD/MSD exciton model, in particular, if the corresponding data²⁰ of the proton entrance channel leading to the same composite system can be included (Sec. IV).

II. EXPERIMENTAL METHOD AND RESULTS

The experiments were performed with α particles accelerated to 28.0–28.5 MeV and 31.5–31.8 MeV, respectively, at the Hamburg Isochronous Cyclotron.

A. The (α, xp) and $(\alpha, x\alpha)$ measurements

Targets consisted of self-supporting metallic foils of high (isotopic) purity ($\geq 99.8\%$); they were $880 \mu\text{g}/\text{cm}^2$ (^{59}Co) and $453 \mu\text{g}/\text{cm}^2$ (^{60}Ni) thick. Protons and α particles were detected with two $\Delta E \times E$ solid state detector telescopes subtending solid angles of typically $200 \mu\text{sr}$. The thickness 29 and $110 \mu\text{m}$ of the respective ΔE detectors allowed an unambiguous particle identification up to the highest energies observed and a low energy cutoff below the evaporation maximum. Reaction angles were varied in 5° and 10° steps between 15° and 160° . The beam was monitored by two Si(Li) detectors sitting at $\pm 25^\circ$ on either side of the projectile direction.

The two linear signals ΔE and $E - \Delta E$ of each telescope were fed into $4k$ analog-to-digital converters (ADC's) and stored on magnetic tape. Dead time corrections determined by means of a reference pulser never exceeded 3% . In forward angle runs the count rate of the α telescope was scaled down by typically 2^N with $N=6$ within a window set on the elastic peak. All runs were extended to guarantee at least 100 proton and α events per MeV in the continuous part ($E^* \geq 3$ MeV) of the spectra. Energy resolution was $\Delta E_p \approx 60-80$ keV and $\Delta E_\alpha \approx 65-110$ keV (FWHM) for the (α, p_0) and elastic scattering group, respectively.

Particle separation was achieved off-line through use of stored $(E - \Delta E)$ and ΔE pulse height information that was corrected for contributions from target contaminations (H,C,O), tailing of the elastic peak, and slit scattering contributions and then converted into double differential cross sections

$d^2\sigma/d\Omega d\epsilon$ in the center-of-mass system assuming single particle emission.

B. The (α, xn) measurements

Metallic self-supporting targets of $3.6 \pm 0.1 \text{ mg}/\text{cm}^2$ were mounted in a thin walled reaction chamber²¹ on top of the "neutron hole" area, a $10 \times 10 \times 4$ m cave in the concrete floor. One of the Si(Li) monitors of the (α, xp) and $(\alpha, x\alpha)$ experiment could be mounted off plane to the (α, xn) scattering chamber at angles between 40° and 50° .

Neutron spectroscopy was performed with time-of-flight (TOF) techniques. The TOF stop signal was derived from the cyclotron radio frequency (RF); the burst frequency was scaled down to ≈ 1.5 MHz by means of an external electrical deflector.²² The neutron TOF detectors were cylindrical NE213 scintillators of 5.1 cm thickness and 10.2 cm diameter, coupled to XP2041 multipliers; they were placed at distances of 6–8 m from the target and heavily shielded with lead, tungsten, and paraffin. The $n-\gamma$ discrimination was performed with the method of Ref. 23. Shadow bars made of 0.7 m canned paraffin that obscured the solid angles of the detectors and provided an attenuation of $\sim 10^3$ could be inserted into the flight path for background measurements.

The TOF electronic is conventional. Low energy biases $E_n^{\text{th}} = 0.96$ MeV were applied to prevent detection of neutrons from preceding bursts. Bias energies have been determined from a calibration with γ sources. The overall time resolution obtained was $\Delta t = 2.0-2.5$ ns (FWHM).

Measurements were performed for typically 6–10 angles between 30° and 150° . Each run was supplemented by an individual background run with a shadow bar. Neutron energy spectra in the c.m. system were obtained by (i) subtracting the background runs, (ii) using the efficiency as calculated with the code HYCALC,²⁴ and (iii) applying the kinematic transformations under the assumption of single particle emission.

C. Absolute cross sections, error estimates

The absolute double differential cross sections $d^2\sigma/d\Omega d\epsilon$ of the (α, α') and (α, p) experiments were derived from target thickness and the charge collected in the Faraday cup, for the (α, n) experiments from the elastic scattering rate observed by the Si(Li) monitor set close to a relative maximum.

Elastic scattering cross sections were obtained in a separate experiment with 28.4 MeV α particles on ^{59}Co , ^{60}Ni . The $\alpha + ^{60}\text{Ni}$ experiment yielded quantitative agreement with the global OM parameters of Budzanowski *et al.*²⁵ and thus, is also consistent with the data of Cowley *et al.*²⁶ for $E_\alpha = 32.3$ MeV from where the reference value $d\sigma/d\Omega(\Theta_{\text{lab}} = 40.7^\circ) = 34.7$ mb/sr was taken. The $\alpha + ^{59}\text{Co}$ experiment yielded $d\sigma/d\Omega(\Theta_{\text{lab}} = 43.0^\circ) = 29.0$ mb/sr.

Relative errors between charged particle spectra obtained under different angles mainly originate from target inhomogeneities and incomplete beam current integration ($\leq 5\%$). Absolute errors of the double differential cross sections predominantly result from statistics ($\leq 10\%$), target thickness ($\leq 9\%$), and sum up to 18% in the region of poorest statistics, but are typically $\leq 15\%$ and $\leq 11-15\%$ for angle integrated differential cross sections.

Relative errors between neutron spectra are mostly due to uncertainties in the background corrections that are estimated to introduce errors up to 10% for $E_n \leq 12$ MeV and all angles; for higher energies and angles they exceed this value and may reach 50% at very backward angles and energies corresponding $E^* \leq 5$ MeV. Absolute error contributions in addition result from the efficiency calculation ($\leq 10\%$) and the elastic scattering cross section used for normalization ($\leq 5\%$). Absolute errors in $d^2\sigma/d\Omega d\epsilon$ are therefore $\leq 15\%$ for $E_n \leq 12$ MeV and may go up to 50% at highest energies and angles. These regions, however, do not contribute substantially to the angle integrated cross sections; we claim errors $\leq 15\%$ for them.

D. Experimental results

Examples of the double differential cross sections for n , p , and α emission are shown in Figs. 1–3 as (i) energy spectra condensed into 0.5 MeV bins for some representative angles, and (ii) angular distributions for bins of 1.0 and 2.2 MeV width, respectively.

Both presentations reveal the influence of non-equilibrium contributions at forward angles and/or high ejectile energies; whereas low energy bins close to the maxima of the spectral distributions show angular distributions that are more (for n and p) or less (for α) symmetric around 90° , the forward peaking becomes the more pronounced the higher the ejectile energy is. However, even at the high energy end of the continuous part of the spectra, the

charged particle angular distributions flatten at very backward angles and in some cases increase again. The backward angle increase is less evident in the neutron data, which is at least in part due to the experimental problem of correct background determination for differential cross sections on the order of $10 \mu\text{b/sr}$.

The general behavior of our data thus is in agreement with the results obtained for proton emission induced by 23, 30, 42, and 55 MeV α particles on ^{59}Co , ^{60}Ni , or other targets of the $A \approx 60$ mass region^{14,15,27} and for neutron emission due to the bombardment of these targets^{13,28} with $E_\alpha \leq 23$ MeV.

In the following section we shall present an interpretation in terms of a statistical model and put emphasis on a consistent description of PE emission in the n , p , and α exit channel. The simultaneous application of both hybrid and exciton PE model is not in contradiction to this program because both approaches have been shown to quantitatively agree if being applied rigorously.²⁹

III. DISCUSSION OF ANGLE INTEGRATED SPECTRA

The angle integrated spectra have been obtained as a sum of the individual spectra with an appropriate solid angle weighting. This procedure introduces some uncertainties, because the very forward emission is underestimated by the data points of the lowest angle, respectively; a more elaborate procedure applying Legendre polynomial fits yielded a $\leq 3\%$ (9%) higher value for the reaction $^{59}\text{Co}(\alpha, xn)$ at $E_n \leq 11$ MeV (17 MeV). The following discussion will be restricted to the (α , nucleon) data, whereas the (α, α') angle integrated spectra will be analyzed elsewhere³⁰ in the framework of the QFS model.³¹

A. The model

Angle integrated particle energy spectra are calculated as an incoherent sum of a PE and the equilibrium (EQ) decay mode. Angular momentum conservation has been taken into account in some cases for the EQ component by choosing the Hauser-Feshbach model instead of the Ewing-Weisskopf formulation, but has been neglected for the PE emission, because its influence on the angle integrated yield is expected to be small³² for the α energies under consideration.

The energy spectrum $d\sigma_y^{\text{PE}}(\epsilon)/d\epsilon$ of particles $y = n, p$ predicted by the hybrid model² is

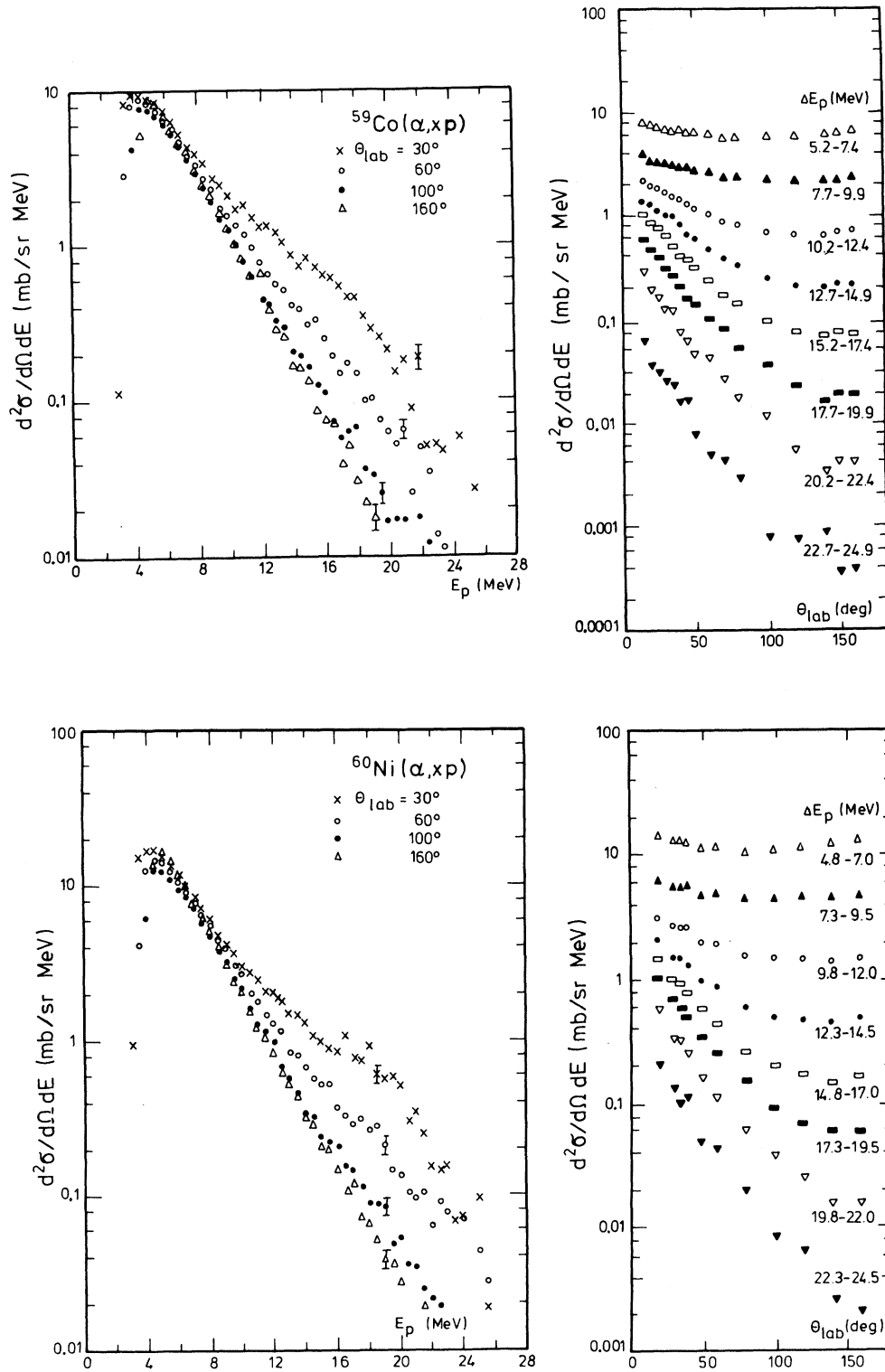


FIG. 1. Proton energy spectra for 0.5 MeV bins, and angular distributions for $\Delta E_p = 2.2$ MeV bins and projectile energies $E_\alpha = 28.5$ (^{59}Co) and 31.8 MeV (^{60}Ni).

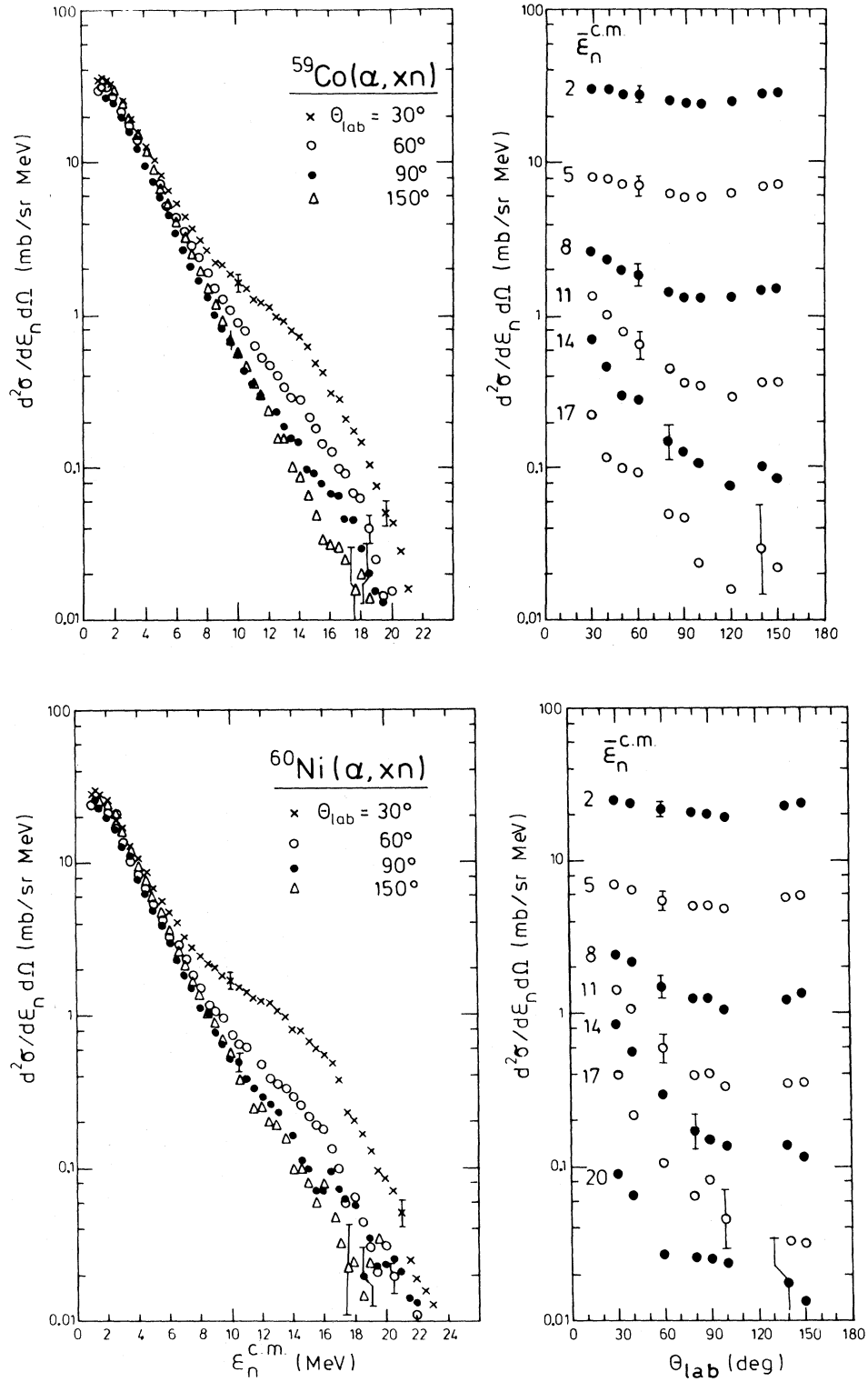
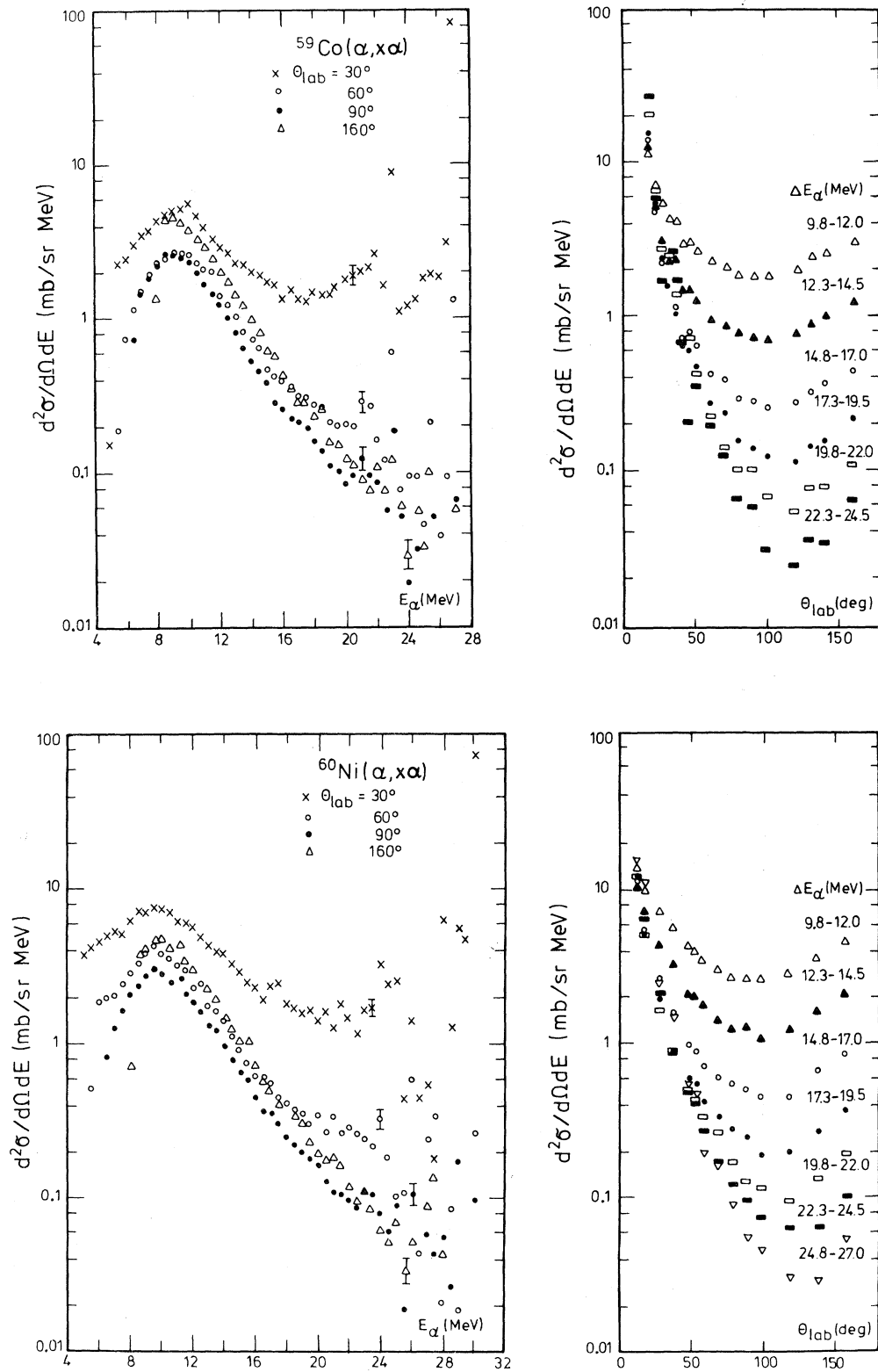


FIG. 2. Neutron energy spectra for 0.5 MeV bins, and angular distributions for 1 MeV bins centered around $\bar{E}_n^{\text{c.m.}}$ (MeV); $E_\alpha = 28.0$ MeV and 31.5 MeV, respectively.

FIG. 3. Same as Fig. 1, but for α particles.

$$\frac{d\sigma_y^{\text{PE}}(\epsilon)}{d\epsilon} = \sigma_R(E_\alpha) \sum_{\substack{n=n_0 \\ \Delta n = +2}}^{\bar{n}} n_y^p \frac{\rho_{n-1}(U)g}{\rho_n(E)} \frac{\lambda_c(\epsilon)}{\lambda_c(\epsilon) + \lambda_+^{\text{NN}}(\epsilon)/k} D_n. \quad (1)$$

Here, σ_R denotes the total reaction cross section at projectile energy E_α ; the sum extends over n exciton state contributions starting from the initial exciton number n_0 up to the equilibrium value \bar{n} . The n exciton state density $\rho_n(E)$ for a total excitation energy E and the $(n-1)$ exciton state density at energy U , such that one nucleon can be emitted with channel energy ϵ , are computed from the single particle state density g with Ericson's formula¹¹; the rates of the competing transitions into continuum $\lambda_c(\epsilon)$ and to states of higher (from n to $n+2$) complexity $\lambda_+^{\text{NN}}(\epsilon)$ are calculated from phase space considerations and from free nucleon-nucleon scattering data corrected for the Pauli principle in nuclear matter, respectively. The mean free path multiplier k has been given the value 1.5 throughout this work. The factor D_n takes into account the depletion of n -exciton states due to preceding PE emission.

The fraction of interactions leading to nucleon PE emission of type y is

$$f_{\text{PE}}^y(E_\alpha) = \frac{1}{\sigma_R(E_\alpha)} \int_0^{\epsilon_{\text{max}}} \frac{d\sigma_y^{\text{PE}}(\epsilon)}{d\epsilon} d\epsilon \quad (2)$$

such that only the remainder $\sigma_R(E) \cdot (1 - f_{\text{PE}}^N - f_{\text{PE}}^\alpha)$ contributes to the formation of the first compound nucleus. This depletion (with f_{PE}^α taken from Refs. 30 and 31) is assumed to be equally distributed over all partial waves in the entrance channel. Multiple PE emission has been neglected.

Deexcitation of the equilibrated system has been followed with the Ewing-Weisskopf model.³³ It takes into account sequential n , p , d , and α emission with the level density of the residual nucleus at excitation energy U given by

$$\rho(U) = \text{const} U^{-5/4} e^{2\sqrt{aU}}. \quad (3)$$

The value $a = A/8 \text{ MeV}^{-1}$ for nuclei with mass number A is used throughout this work. For testing purposes the Ewing-Weisskopf calculation has been replaced by a full statistical model³⁴ calculation including angular momentum conservation and deexcitation by γ emission. Of particular interest for the present work is the level density applied:

$$\rho(U, I) = \rho(U) \cdot \frac{1}{2\sigma^2} (2I+1) \times \exp \left[-\frac{I(I+1)}{2\sigma^2} \right], \quad (4)$$

with

$$\rho(U) = \text{const} \frac{\exp(2[a(U-\Delta)]^{1/2})}{(U-\Delta+t)^{5/4}}. \quad (5)$$

Here, t is the thermodynamic temperature given by $U-\Delta = at^2 - t$; a and Δ are level density parameter and fictive ground state position, and were taken from Ref. 35. For the spin cutoff parameter σ the value for a rigid rotator (with $r_0 = 1.25 \text{ fm}$) is used. Further details are given in Ref. 12.

B. The initial exciton number n_0

For α particles some preference for $n_0=3$ was found¹³ from neutron energy spectra of (α, n) reactions with $E_\alpha=20 \text{ MeV}$ projectiles on a variety of targets with masses $A=54-124$. Hybrid model analyses of (α, p) spectra for $E_\alpha=23 \text{ MeV}$ reactions on $A=54-63$ targets, that took into account pairing corrections in the expressions for the exciton state densities,¹⁴ yielded $n_0=4$ ($n_n=2$, $n_p=2$, $n_h=0$) for all even-even, $n_0=5$ (2, 3, 0) for odd Z , and $n_0=5$ (3, 2, 0) for odd N targets. This result indicates a decomposition of the projectile into four nucleons which, together with the unpaired nucleons, make up the initial exciton configuration. It is only in partial agreement with the analysis of (α, p) spectra for $E_\alpha=55 \text{ MeV}$ projectiles on several targets with $A=51-197$; here, in the framework of hybrid and exciton model, again the parameter $n_0=5$ was found¹⁵ for all odd Z targets. However, $n_0=4$ was deduced not only for all even-even targets but also for the odd N target ${}^{57}_{26}\text{Fe}$. This result was obtained by applying exciton state densities without pairing corrections for the odd-even character of the residual nuclei following PE emission.

There are two possible explanations for this particular case ${}^{57}\text{Fe}(\alpha, p)$. First, n_0 may be dependent mainly on the exit channel and less on the composite system; second, the unexpected value for n_0 , as already pointed out in Ref. 15, is necessary to compensate for the shortcomings, namely the lack of pairing correction, of the state density *ansatz*. The first explanation is obviously in conflict with the PE picture that equilibration proceeds through two particle interactions, because in α induced reactions there is no reason to favor an initial interaction with an unpaired proton over that with an unpaired neu-

tron. In order to examine the second explanation, the introduction of a shift Δ that replaces the excitation energy U in Eq. (1) by $U - \Delta$ shall be considered now.

In the back shifted Fermi gas model the shift Δ_{ee} of the fictive ground state as compared with the actual one is slightly positive for even-even nuclei, i.e., the pairing and shell corrections to the equidistant spacing model do about cancel.^{35,36} Accordingly the shifts Δ_{0e} or Δ_{e0} for odd mass nuclei and Δ_{00} for odd-odd nuclei are negative, they differ from Δ_{ee} by roughly the pairing energies as determined from the masses of the corresponding adjacent nuclei. Average values in the mass region $A \approx 60$ that have been successfully applied in particle evaporation calculations and also in PE calculations for (α, p) data from 23 MeV projectiles,¹⁴ are (Ref. 35) $\Delta_{ee} = 0.6$ MeV, $\Delta_{e0} = \Delta_{0e} = -0.7$ MeV, and $\Delta_{00} = -2$ MeV. Comparisons of total level densities generated from the equidistant spacing model with those from realistic single-particle level schemes provide some theoretical justification for the back shift parametrization.³⁷

In the conventional shifted Fermi gas model³⁸ the fictive ground state is assumed to coincide with the actual one for odd-odd nuclei (i.e., $\Delta_{00}^* = 0$), and for odd mass and even-even nuclei the ground states are shifted upward by the pairing energies; here, the values $\Delta_{0e}^* = 1.3$ MeV and $\Delta_{ee}^* = 2.6$ MeV will be used.³⁵ Owing to this ground state convention the conventionally shifted level density is bound to deviate more from experimental data than the back shifted ones; in the latter case the parameters a and Δ of Eqs. (4) and (5) are derived³⁵ from a best fit to the level densities obtained from level counting and neutron resonance data, i.e., for the excitation energy region $U \leq 10$ MeV relevant for the PE contribution of the spectra under consideration.

On the other hand it is known that both kinds of shift corrections cause problems with experimental data that are sensitive to the position of the reaction threshold³⁹ or very low residual excitation energy. Furthermore, it should be pointed out that *partial* state densities $\rho_{n-1}(U)$ are entering in Eq. (1) and conclusions drawn for the applicability of shifts in total densities may not apply. In fact, it has been shown,⁴⁰ that partial state densities calculated from realistic level schemes may differ considerably at low excitation energies from those of the equidistant spacing model and may require shifts Δ for compensation that depend on n . The discrepancies, however, were found to decrease with increasing excitation number n ; therefore the result⁴¹ that the con-

ventional shift is adequate for the PE contribution (with $n_0 = 3$) in (p, n) spectra, does not necessarily rule out the back shift for α -induced reactions characterized by $n_0 = 4$ or 5. We shall therefore consider both possibilities and return first to the case $^{57}\text{Fe}(\alpha, p)^{60}\text{Co}$.

As the residual nucleus ^{60}Co is an odd-odd one, the conventional shift does not modify the shape of the proton spectrum (i.e., $n_0 = 4$), but only enhances the absolute values on the account of the neutron exit channel, whereas the back shift correction enhances the excitation energy, and qualitatively this shift can be sufficient to increase the best fit value of n_0 by one unit (i.e., $n_0 = 5$) as was found in Ref. 42 for (p, n) reactions. The value $n_0 = 5$ was also found for $^{57}\text{Fe}(\alpha, n)^{60}\text{Ni}$ (Ref. 13); for this reaction the conventional shift would decrease the effective excitation energy and therefore lead to a fit with $n_0 < 5$.

A more quantitative conclusion may be drawn from our $(\alpha, \text{nucleon})$ data. Calculations without shift corrections yield the best agreement for $\alpha + ^{60}\text{Ni}$ with $n_0 = 4$, see Fig. 4. The results for $\alpha + ^{59}\text{Co}$ indicate $n_0 = 4$ for the (α, xn) reaction and $n_0 = 5$ for the (α, xp) reaction. This discrepancy can be removed by introducing a shift correction.

The back shift corrected calculations are shown in Fig. 4. For the $^{59}\text{Co}(\alpha, xp)$ case the modification is moderate, because the residual nucleus ^{62}Ni is even-even. The proton yield is reduced because the back shift $\Delta_{00} < 0$ for the $^{59}\text{Co}(\alpha, xn)$ reaction with the odd-odd residual nucleus ^{62}Cu enhances the neutron PE emission. In addition the calculated neutron spectrum now extends to higher energies; as a consequence the best fit is obtained with $n_0 = 5$. The back shift correction thus leads to $n_0 = 4$ for $\alpha + ^{60}\text{Ni}$ and $n_0 = 5$ for $\alpha + ^{59}\text{Co}$ consistently for both exit channels and in agreement with the odd-even character of the reaction system, cf. Table I.

The results of a calculation with conventional shift Δ^* are compiled in Fig. 5. Whereas for $\alpha + ^{60}\text{Ni}$ the best fit value $n_0 = 4$ still holds, the system $\alpha + ^{59}\text{Co}$ now also shows a preference for $n_0 = 4$ in both exit channels and $n_0 = 5$ is incompatible with the data. The extent of agreement is comparable with that for $n_0 = 5$ in the case of a back shift correction.

Therefore, if $n_0 = 4$ and 5 were equally acceptable for an odd-even reaction system like $\alpha + ^{59}\text{Co}$, none of the two shift corrections could clearly be ruled out on the basis of the calculations presented. If, however, the indications for $n_0 = 5$ for odd-even systems found in (α, xp) spectra and excitation func-

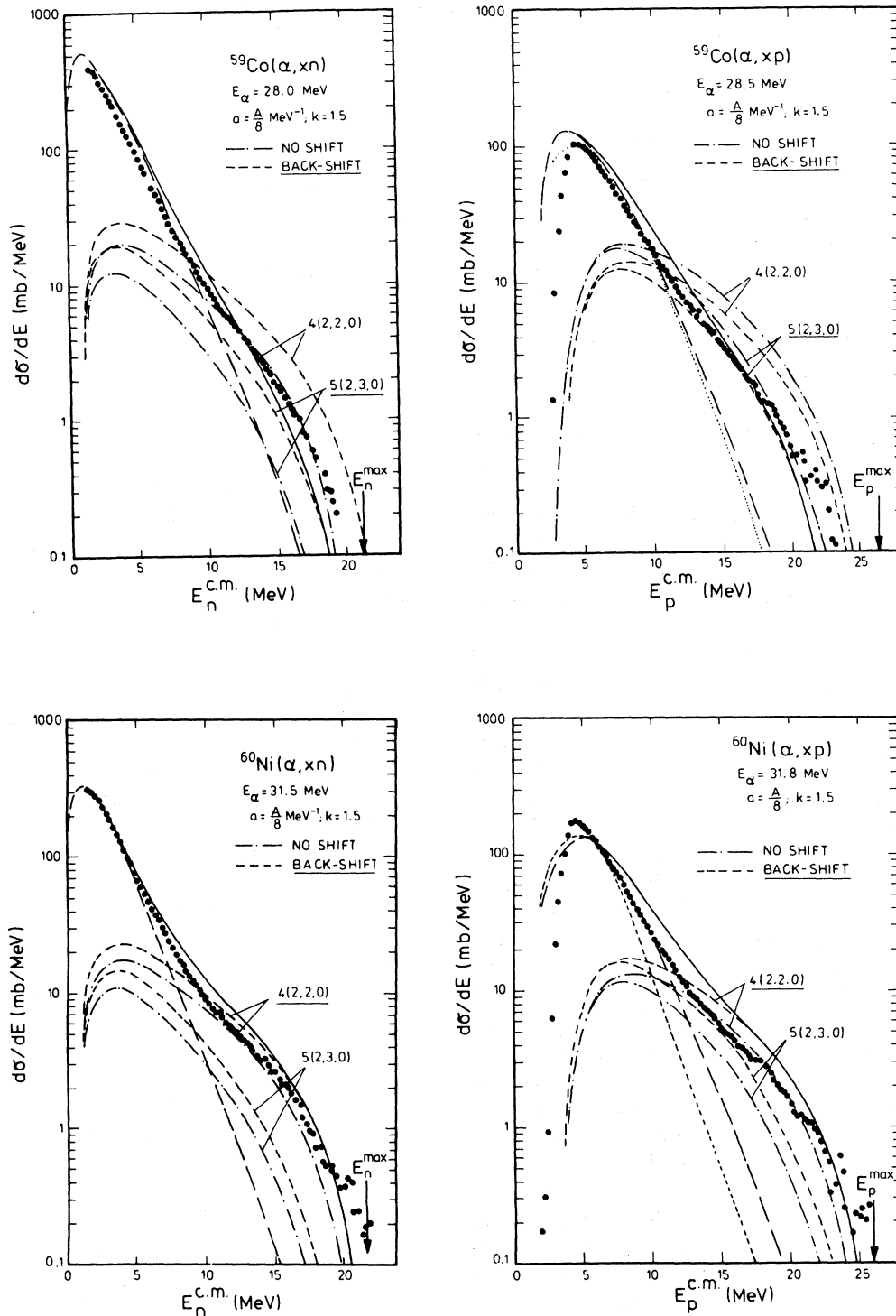


FIG. 4. Angle integrated nucleon spectra. The arrows indicate the Q -value limits. Calculations: Hybrid model with ground state back shift Δ for (1) Initial configuration $n_0=4(2, 2, 0)$. (2) Initial configuration $n_0=5(2, 3, 0)$. (3) Ewing-Weisskopf model with back-shifted ground state (long dashed). (4) Hauser-Feshbach model (short dashed). (5) Sum of (3) with (2) or (1) (as underlined), respectively (solid lines). (6) Calculations (1) and (2) without shift Δ . The lines from calculations (1), (2), and (6) are dashed as indicated in the figure.

TABLE I. Correlation of odd-even character with initial exciton number for calculation including back shift correction.

Reaction	Target + α		Residual nucleus		$n_0(n_n, n_p, n_h)$
	Z	N	Z	N	
$^{59}\text{Co}(\alpha, n)^{62}\text{Cu}$	odd	even	odd	odd	5(2, 3, 0)
$^{59}\text{Co}(\alpha, p)^{62}\text{Ni}$	odd	even	even	even	5(2, 3, 0)
$^{60}\text{Ni}(\alpha, n)^{63}\text{Zn}$	even	even	even	odd	4(2, 2, 0)
$^{60}\text{Ni}(\alpha, p)^{63}\text{Cu}$	even	even	odd	even	4(2, 2, 0)

tions of α -induced reactions^{14,15,43} are also taken into account, we deduce a preference for the back shift correction, and *vice versa*.

Finally it should be noted, that the comparison of Figs. 4 and 5 demonstrates the sensitivity of the calculations to a general variation in Δ , because $\Delta^* - \Delta \approx 2$ MeV for odd-odd, odd mass, and even-even systems. Attempts to obtain a consistent description without shift correction by varying k between the values 1 and 4 failed⁴⁴; the $\alpha + ^{59}\text{Co}$ exit channels cannot be fitted simultaneously with $n_0 = 5$ nor with $n_0 = 4$ and any value $k \geq 1$.

The comparison so far has been concentrated on the shape and absolute magnitude of the nucleon energy spectra in the region extending from ~ 3 MeV below the Q value limit to about 10 MeV ejectile energy, where PE and EQ contributions become comparable. In this region the EQ contribution is sufficiently small, such that deviations between the Ewing-Weisskopf and the full statistical model calculation, though they may reach a factor of 2 (Fig. 4), have no influence on the interpretation in terms of the PE model under discussion. At about 10 MeV nucleon energy, however, the calculated total spectrum starts to be sensitive to details of the EQ contribution and a replacement of calculation (3) by (4) in Fig. 4 would improve the fit. In addition, the fraction of contributions to the PE decay due to exciton numbers $n > n_0$ increases and therefore, approximations leading to the depletion factor D_n in Eq. (1) instead of a complete bookkeeping on exciton state occupation may also be responsible²⁹ for the slight discrepancy in the 10 MeV region.

IV. DISCUSSION OF ANGULAR DISTRIBUTIONS

The quantum mechanical treatment of the equilibration process by Feshbach *et al.*⁸ leads to a dis-

tribution among two modes of PE emission, namely the statistical multistep compound (MSC) emission proceeding only through particle bound states, and the multistep direct (MSD) emission involving states with at least one unbound particle. The angular distributions of the emitted particles show characteristic differences; whereas the MSC emission is symmetric around 90° , the MSD component is peaked in the forward direction.

The exciton model has recently¹⁸ been extended by implementation of the ideas of MSC and MSD particle emission with an appropriate modification of the definition of MSC processes, whereas the MSD definition was retained. It then allows us to divide the PE cross section into one part which is due to an equilibration through particle unbound states and is again referred to as MSD contribution; its angular distribution is expected to be forward peaked; and into the complementary MSC part.

The shapes of the angular distributions for both components have been derived phenomenologically.¹⁹ For this purpose a considerable amount of experimental angular distributions for nucleons, deuterons, and both He isotopes in the entrance and the exit channel, and a broad range of projectile and ejectile (y) energies has been fitted with the Legendre polynomial $P_l(\cos\Theta)$ expansion

$$\frac{d^2\sigma_y}{d\Omega d\epsilon} = a_0^{\text{MSD}} \sum_{l=0}^{l_{\text{max}}} \frac{a_l}{a_0} P_l(\cos\Theta) + a_0^{\text{MSC}} \sum_{\substack{l=0 \\ \Delta l=2}}^{l_{\text{max}}} \frac{a_l}{a_0} P_l(\cos\Theta). \quad (6)$$

Here, a_0^{MSD} and a_0^{MSC} are taken from the extended exciton model and fulfill the relation

$$4\pi(a_0^{\text{MSD}} + a_0^{\text{MSC}}) = 4\pi a_0 = d\sigma_y^{\text{PE}}(\epsilon)/d\epsilon;$$

the coefficients $b_l = a_l/a_0$ are the result of the fit-

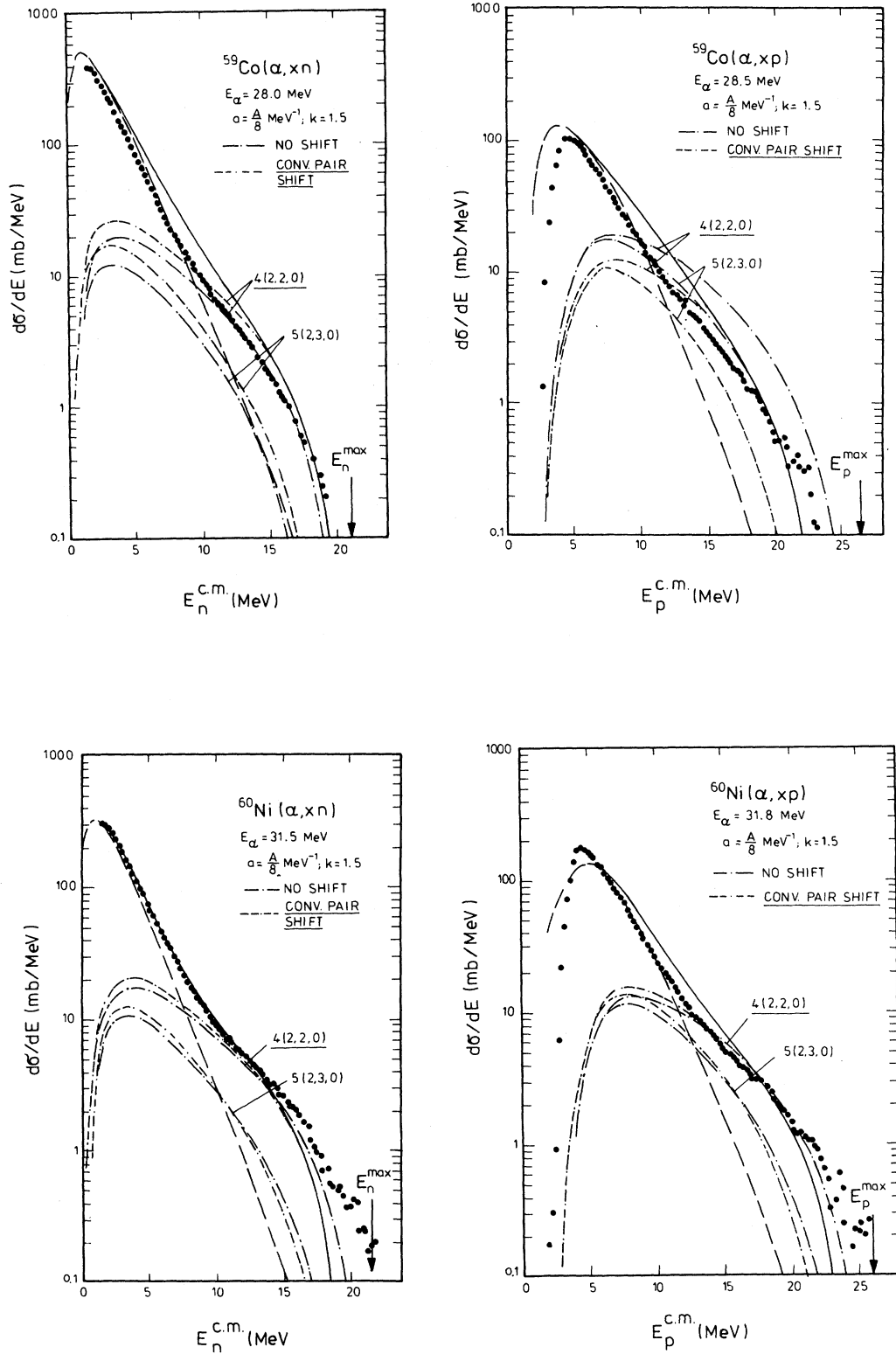


FIG. 5. Same as Fig. 4, but calculations (1) and (2) performed with conventional shift correction Δ^* . The calculations (6) are repeated for reference.

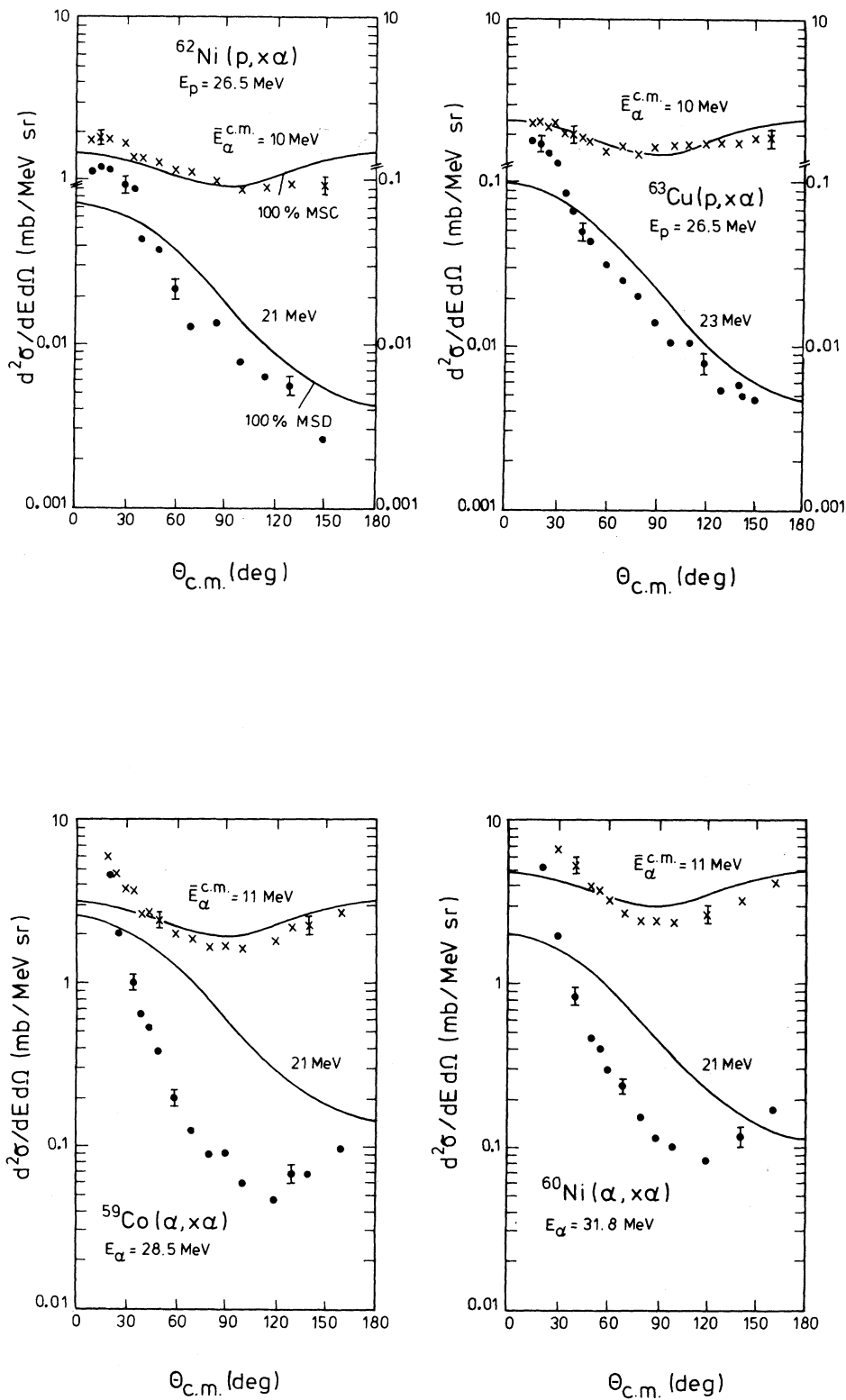


FIG. 6. Angular distributions of α particles emitted during deexcitation of ^{63}Cu ($E^* = 32.4 \pm 0.4$ MeV) and ^{64}Zn ($E^* = 33.8 \pm 0.4$ MeV) for two energies. Solid lines are normalized MSD/MSD exciton model calculations.

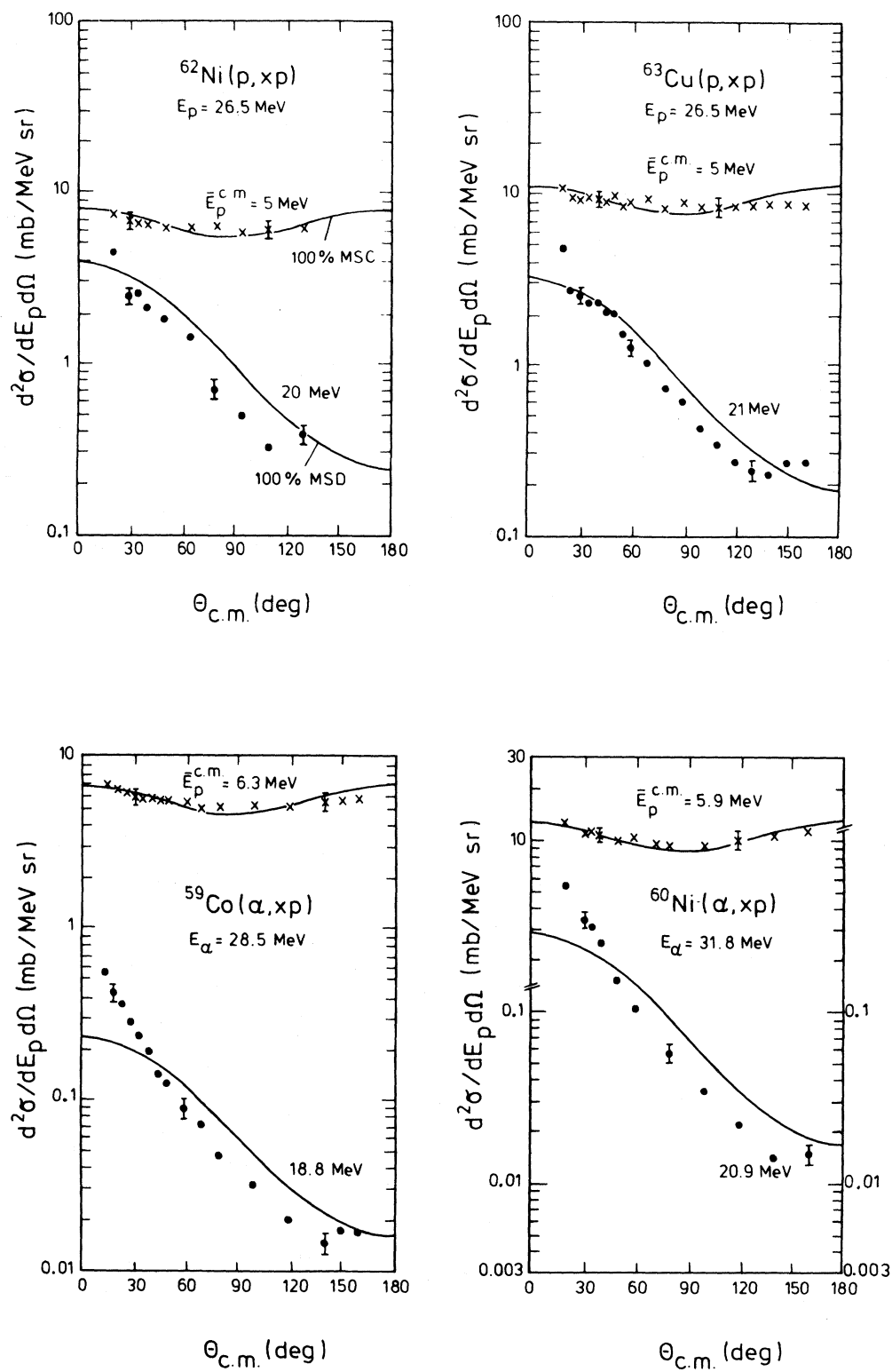


FIG. 7. Same as Fig. 6, but for protons.

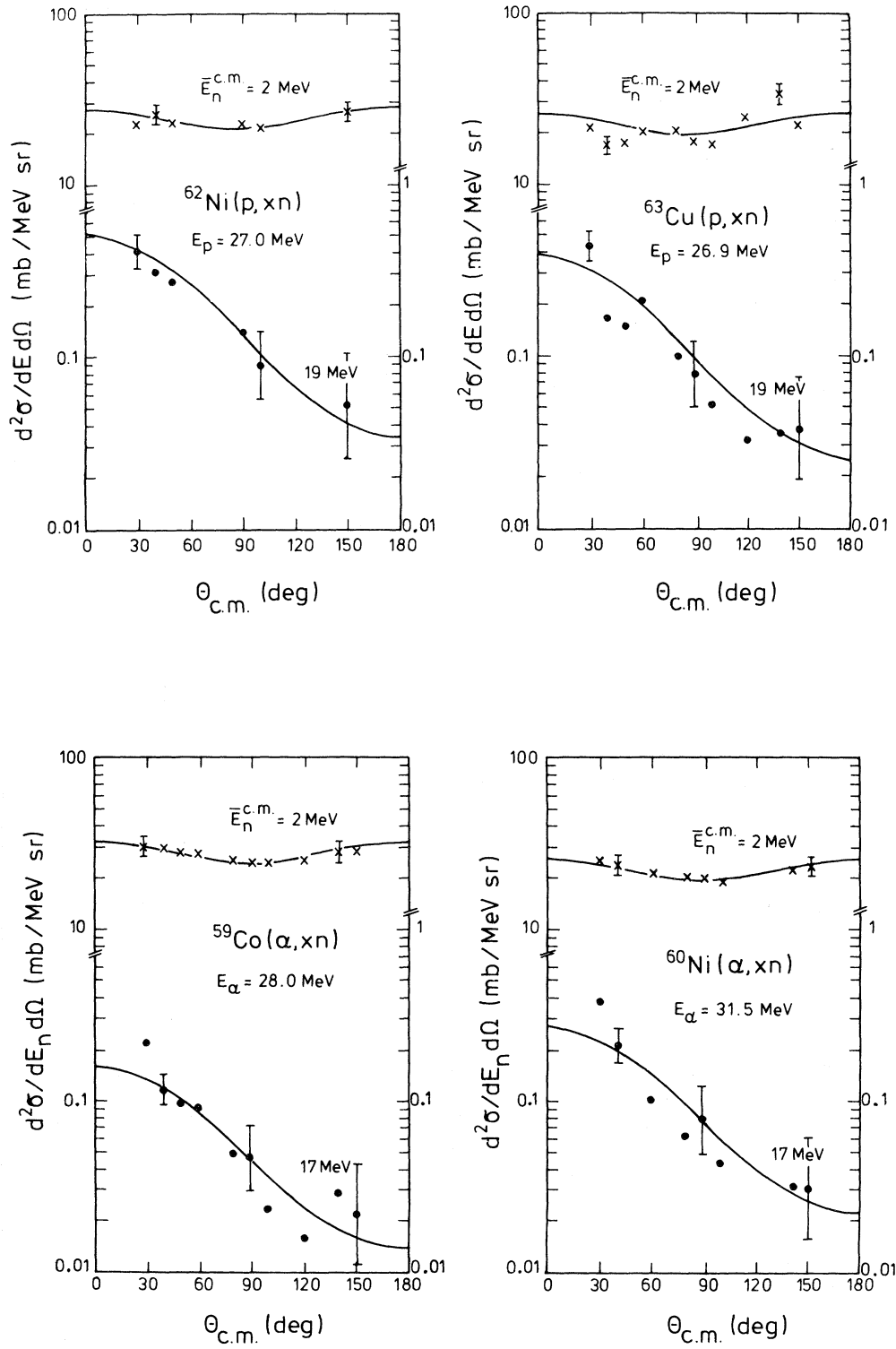


FIG. 8. Same as Fig. 6, but for neutrons.

ting procedure.

It turned out that the data analyzed are in agreement with (i) identical coefficients b_l for both (MSC and MSD) components and (ii) an upper limit $l_{\max}=8$ (for projectiles with energies up to 62 MeV and mass numbers up to 4). Inspection of the coefficients b_l showed that for ejectile energies with dominating MSD contribution the shape of the angular distribution is almost exclusively determined by ϵ such that they could be parametrized as

$$b_l(\epsilon) = \frac{(2l+1)}{1 + \exp[A_l(B_l - \epsilon)]}, \quad (7)$$

with universal coefficients A_l and B_l .¹⁹ In particular, the shapes are predicted to be not dependent on (1) projectile energy, (2) projectile mass number, (3) target mass number, and (4) type of outgoing particle.

Our (α, xn) , (α, xp) , and $(\alpha, x\alpha)$ data are particularly suited to test prediction (4). In order to check prediction (2) we include in the comparison the $p + {}^{62}\text{Ni}$, ${}^{63}\text{Cu}$ data from Ref. 20 that were taken with 26.5 and 27 MeV projectiles leading to the same reaction systems and, within ± 0.4 MeV, to the same excitation energies as the α induced reactions.

The data are presented in Figs. 6–8 as a comparison of two different entrance channels with the same type of outgoing particle. Two ejectile energies ϵ have been chosen, a lower one which is at most 3 MeV above the evaporation maximum and well above the detection threshold, and a higher one corresponding to an excitation energy of at least 3 MeV left in the residual nucleus. The results of Eqs. (6) and (7) are shown with $4\pi a_0$ being normalized to the angle integrated yield $d\sigma/d\epsilon$ to facilitate a good comparison of the shapes. For simplification we have assumed 100% MSC (MSD) contribution at the lower (higher) energy.

At the low energies the data show the expected symmetry around 90° ; the excess of the $(\alpha, x\alpha)$ yield at forward angles is neither observed for the $(p, x\alpha)$ nor for the (p, xp) data. If we exclude systematic experimental errors for this excess, it must be considered an indication of a higher MSD contribution at 10–11 MeV ejectile energy than in the $(p, x\alpha)$ reaction. This difference is more pronounced for the high energy data. Whereas the $(p, x\alpha)$ angular distributions show additional peaking for $\Theta < 30^\circ$ and are in fair agreement with the phenomenological

model for angles $\Theta > 30^\circ$, the $(\alpha, x\alpha)$ angular distributions have a much more pronounced excess for $\Theta < 30^\circ$ and show a steeper descent and a minimum at 120° . The increase at backward angles may be in part due to the neglect of the MSC contribution which then would be about 1 mb/MeV (or 10% of the total $d\sigma/d\epsilon$) to account for the observed yield. This value is to be compared with $d\sigma^{\text{HF}}/d\epsilon = 0.4$ (< 0.1) mb/MeV for ${}^{60}\text{Ni}(\alpha, x\alpha)$ [${}^{59}\text{Co}(\alpha, x\alpha)$] predicted by the Hauser-Feshbach calculation. The MSC contribution, however, cannot be responsible for the discrepancy at $\Theta < 120^\circ$, because it is too small and flattens the shape of the angular distribution.

V. CONCLUSIONS

The angle integrated nucleon spectra from reactions of 28 and 31.2 MeV α particles with ${}^{59}\text{Co}$ and ${}^{60}\text{Ni}$, respectively, can be described consistently in terms of a combined PE-EQ calculation if the excitation energy U in the residual systems is replaced by an effective excitation energy $U - \Delta$. Application of a back shift Δ leads to $n_0 = 4$ for the system $\alpha + {}^{60}\text{Ni}$ and $n_0 = 5$ for $\alpha + {}^{59}\text{Co}$, whereas the conventional shift Δ^* allows a fit with $n_0 = 4$ in both cases. No distinction between these two types of pairing correction is possible on the basis of this comparison alone; the arguments given in Sec. III B, however, lead us to favor the back shift correction.

The angular distributions, in particular those of the $(\alpha, x\alpha)$ data in comparison with the $(p, x\alpha)$ data, indicate that their shapes depend on the type of projectile with a preference for forward emission for the α -induced reactions. This conclusion is supported by the high energy data for nucleon emission (Figs. 7 and 8) which also show forward emission more intense for α than for the corresponding proton induced reactions and than predicted by the model. At higher angles their shapes are similar to those of the $(p, x\alpha)$ data and in so far support the independence from the type of ejectile predicted in Ref. 19.

ACKNOWLEDGMENTS

We thank Mr. H. Krause for his help with some experimental problems. This work was supported by the Bundesministerium für Forschung und Technologie.

- *Permanent address: Institut de Fizica si Inginerie Nucleara, Bucharest, Romania.
- ¹E. Gadioli and E. Gadioli Erba, Nucl. Instrum. Methods 146, 265 (1977).
 - ²M. Blann and A. Mignerey, Nucl. Phys. A186, 245 (1972).
 - ³G. Mantzouranis, H. A. Weidenmüller, and D. Agassi, Z. Phys. A 276, 145 (1976).
 - ⁴G. Mantzouranis, Phys. Lett. 63B, 25 (1976).
 - ⁵H. Machner, Phys. Lett. 86B, 129 (1979).
 - ⁶J. M. Akkermans, J. M. H. Gruppelaar, and G. Reffo, Phys. Rev. C 22, 73 (1980).
 - ⁷T. Tamura, T. Udagawa, D. H. Feng, and K. K. Kan, Phys. Lett. 66B, 109 (1977).
 - ⁸H. Feshbach, A. Kerman, and S. Koonin, Ann. Phys. (N.Y.) 125, 429 (1980).
 - ⁹H. C. Chiang and J. Hüfner, Nucl. Phys. A349, 466 (1980).
 - ¹⁰J. Bisplinghoff, J. Ernst, R. Löhr, T. Mayer-Kuckuk, and P. Meyer, Nucl. Phys. A269, 147 (1976).
 - ¹¹M. Blann, A. Galonsky, R. R. Doering, D. M. Patterson, and F. E. Serr, Nucl. Phys. A257, 15 (1976).
 - ¹²H. H. Bissem, R. Georgi, W. Scobel, J. Ernst, M. Kaba, J. Rama Rao, and H. Strohe, Phys. Rev. C 22, 1468 (1980).
 - ¹³A. Alevra, R. Dumitrescu, I. R. Lukas, M. T. Magda, D. Plostinaru, E. Trutia, N. Chevarier, A. Chevarier, A. Demeyer, and T. M. Duc, Nucl. Phys. A209, 557 (1973).
 - ¹⁴A. Alevra, M. Duma, I. R. Lukas-Koch, M. T. Magda, H. E. Nistor, A. Chevarier, N. Chevarier, A. Demeyer, G. Hollinger, and T. M. Duc, Nucl. Phys. A265, 376 (1976).
 - ¹⁵A. Chevarier, N. Chevarier, A. Demeyer, G. Hollinger, P. Pertosa, and T. M. Duc, Phys. Rev. C 8, 2155 (1973).
 - ¹⁶R. Bonetti, L. Colli-Milazzo, A. de Rosa, G. Inghima, E. Perillo, M. Sandoli, and F. Shahin, Phys. Rev. C 21, 816 (1980).
 - ¹⁷R. Bonetti, M. Camnasio, L. Colli-Milazzo, and P. E. Hodgson, Phys. Rev. C 24, 71 (1981).
 - ¹⁸C. Kalbach, Phys. Rev. C 23, 124 (1981); 23, 2798 (1981).
 - ¹⁹C. Kalbach and F. M. Mann, Phys. Rev. C 23, 112 (1981).
 - ²⁰W. Scobel, H. H. Bissem, J. Friese, H. Krause, H. J. Langanke, R. Langkau, P. Plischke, and R. Wien, Proceedings of the International Workshop on Reaction Models for Continuous Spectra of Light Particles, Bad Honnef, 1978; H. H. Bissem, J. Friese, H. Krause, H. J. Langanke, R. Langkau, P. Plischke, R. Scherwinski, W. Scobel, and R. Wien, Report HH79-01, Institut für Experimentalphysik, Hamburg, 1979.
 - ²¹P. Plischke, W. Scobel, and M. Bormann, Z. Phys. A 281, 245 (1977).
 - ²²H. Krause, R. Langkau, and N. Schirm, Nucl. Instrum. Methods 134, 15 (1976).
 - ²³J. M. Adams and G. White, Nucl. Instrum. Methods 136, 459 (1976).
 - ²⁴E. Magiera, M. Bormann, W. Scobel, and P. Heiss, Nucl. Phys. A246, 413 (1975).
 - ²⁵A. Budzanowski, H. Dabrowski, L. Freindl, K. Grotowski, S. Micek, R. Planeta, A. Strzalkowski, M. Bosman, P. Leleux, P. Macq, J. P. Meulders, and C. Pirart, Phys. Rev. C 17, 951 (1978).
 - ²⁶A. A. Cowley, P. M. Cronje, G. Heymann, S. J. Mills, and J. C. van Staaden, Nucl. Phys. A229, 256 (1974).
 - ²⁷R. W. West, Phys. Rev. 141, 1033 (1966).
 - ²⁸M. T. Magda, A. Alevra, I. R. Lukas, D. Plostinaru, E. Trutia, and M. Molea, Nucl. Phys. A140, 23 (1970).
 - ²⁹J. Ernst and J. Rama Rao, Z. Phys. A 281, 129 (1977).
 - ³⁰R. Scherwinski, J. Friese, C. Heidorn, and W. Scobel, Progress Report on Nuclear Data Research in the Federal Republic of Germany 222 (U), 1981, Vol. V (unpublished).
 - ³¹A. Mignerey, M. Blann, and W. Scobel, Nucl. Phys. A273, 125 (1976).
 - ³²H. H. Bissem and W. Scobel, Nukleonika (in press).
 - ³³M. Blann, OVERLAID ALICE, US ERDA Report COO-3494-29, 1976 (unpublished).
 - ³⁴M. Uhl, Nucl. Phys. A184, 253 (1972).
 - ³⁵W. Dilg, W. Schantl, H. Vonach, and M. Uhl, Nucl. Phys. A217, 269 (1973).
 - ³⁶H. Vonach and M. Hille, Nucl. Phys. A127, 289 (1969).
 - ³⁷F. C. Williams, G. Chan, and J. R. Huizenga, Nucl. Phys. A187, 225 (1972).
 - ³⁸E. Erba, U. Facchini, and E. Saetta-Menichella, Nuovo Cimento 22, 1237 (1961).
 - ³⁹M. Bormann, H. K. Feddersen, H. H. Hölscher, W. Scobel, and H. Wagener, Z. Phys. A 277, 203 (1976).
 - ⁴⁰K. Albrecht and M. Blann, Phys. Rev. C 8, 1481 (1973).
 - ⁴¹S. M. Grimes, J. D. Anderson, and C. Wong, Phys. Rev. C 13, 2224 (1976).
 - ⁴²S. M. Grimes, J. D. Anderson, J. W. McClure, B. A. Pohl, and C. Wong, Phys. Rev. C 7, 343 (1973).
 - ⁴³M. Blann, Annu. Rev. Nucl. Sci. 25, 123 (1975).
 - ⁴⁴H. Machner, Z. Phys. A 302, 125 (1981).